

Supplemental material

S1 Corrections for hygroscopic growth

A dryer was used prior to sampling with the SMPS at the Amphitrite Point site. To allow comparison with other measurements, the SMPS data at Amphitrite Point were corrected for hygroscopic growth using the following equation
5 (Hämeri et al., 2000):

$$gf(RH) = \frac{D_{p,RH}}{D_{p,dry}}, \quad (S1)$$

where $gf(RH)$ is the hygroscopic growth factor at measured relative humidity (RH); $D_{p,RH}$ is the particle diameter at measured RH; $D_{p,dry}$ is the dry particle diameter. The hygroscopic growth factor was calculated with the numerical model developed by Ming and Russell (2001) assuming the sampled aerosol consisted of sea spray aerosol with a 30% organic
10 mass content, following the assumption made in DeMott et al. (2016). This assumption results in growth factors consistent with measurements in the marine boundary layer (Zhou et al., 2001) and a hygroscopicity parameter, κ , consistent with measurements at Amphitrite Point during the same campaign (Yakobi-Hancock et al., 2014).

S2 Conversion of mobility diameter to aerodynamic diameter

The SMPS measured mobility diameter rather than aerodynamic diameter, while both APS and MOUDI measured
15 aerodynamic diameter. To allow comparison between the SMPS data, the APS data and the INP data, the mobility diameter, D_m , measured by the SMPS (corrected for hygroscopic growth first for Amphitrite Point data as discussed above) was converted to aerodynamic diameter, D_{ae} , using the following equation (Khlystov et al., 2004):

$$D_{ae} = \sqrt{\frac{\rho_{p,RH}}{\chi \rho_o}} D_m, \quad (S2)$$

where χ is the dynamic shape factor that accounts for the non-spherical particle shape; ρ_o is the unit density of 1 g cm^{-3} ; and
20 $\rho_{p,RH}$ is the particle density at measured RH. In all cases, we assumed a dynamic shape factor of 1. The particle density at measured RH, $\rho_{p,RH}$, was calculated using the equation below:

$$\rho_{p,RH} = \rho_w + (\rho_{p,dry} - \rho_w) \frac{1}{gf^3}, \quad (S3)$$

where ρ_w is the density of water; $\rho_{p,dry}$ is the density of dry particles; gf is the growth factor. The gf was calculated as discussed in Sect. S1, and the $\rho_{p,dry}$ was calculated using the same assumption that the sampled aerosol consisted of sea
25 spray aerosol with a 30% organic mass content.

References:

- DeMott, P. J., Hill, T. C. J., McCluskey, C. S., Prather, K. A., Collins, D. B., Sullivan, R. C., Ruppel, M. J., Mason, R. H., Irish, V. E., Lee, T., Hwang, C. Y., Rhee, T. S., Snider, J. R., McMeeking, G. R., Dhaniyala, S., Lewis, E. R., Wentzell, J. J. B., Abbatt, J., Lee, C., Sultana, C. M., Ault, A. P., Axson, J. L., Diaz Martinez, M., Venero, I., Santos-Figueroa, G., Stokes, M. D., Deane, G. B., Mayol-Bracero, O. L., Grassian, V. H., Bertram, T. H., Bertram, A. K., Moffett, B. F. and Franc, G. D.: Sea spray aerosol as a unique source of ice nucleating particles, *Proc. Natl. Acad. Sci.*, 113(21), 5797–5803, doi:10.1073/pnas.1514034112, 2016.
- Hämeri, K., Väkevää, M., Hansson, H. C. and Laaksonen, A.: Hygroscopic growth of ultrafine ammonium sulphate aerosol measured using an ultrafine tandem differential mobility analyzer, *J. Geophys. Res.*, 105(D17), 22231–22242, doi:10.1029/2000JD900220, 2000.
- Khlystov, A., Stanier, C. and Pandis, S. N.: An algorithm for combining electrical mobility and aerodynamic size distributions data when measuring ambient aerosol, *Aerosol Sci. Technol.*, 38(S1), 229–238, doi:10.1080/02786820390229543, 2004.
- Ming, Y. and Russell, L. M.: Predicted hygroscopic growth of sea salt aerosol, *J. Geophys. Res.*, 106(D22), 28259–28274, doi:10.1029/2001JD000454, 2001.
- Niemand, M., Möhler, O., Vogel, B., Vogel, H., Hoose, C., Connolly, P., Klein, H., Bingemer, H., DeMott, P., Skrotzki, J. and Leisner, T.: A Particle-Surface-Area-Based Parameterization of Immersion Freezing on Desert Dust Particles, *J. Atmos. Sci.*, 69(10), 3077–3092, doi:10.1175/JAS-D-11-0249.1, 2012.
- Yakobi-Hancock, J. D., Ladino, L. A., Bertram, A. K., Huffman, J. A., Jones, K., Leaitch, W. R., Mason, R. H., Schiller, C. L., Toom-Saunty, D., Wong, J. P. S. and Abbatt, J. P. D.: CCN activity of size-selected aerosol at a Pacific coastal location, *Atmos. Chem. Phys.*, 14(22), 12307–12317, doi:10.5194/acp-14-12307-2014, 2014.
- Zhou, J., Swietlicki, E., Berg, O. H., Aalto, P. P., Hämeri, K., Nilsson, E. D. and Leck, C.: Hygroscopic properties of aerosol particles over the central Arctic Ocean during summer, *J. Geophys. Res.*, 106(D23), 32111–32123, 2001.

25

30

Table S1. The correction factors $f_{nu,1\text{ mm}}$ and $f_{nu,0.25-0.1\text{ mm}}$ for MOUDI stages 2-8 when using substrate holders. The uncertainty in $f_{nu,1\text{ mm}}$ is given as the standard deviation.

MOUDI Stages	$f_{nu,1\text{ mm}}$	$f_{nu,0.25-0.1\text{ mm}}$
2	0.74, +0.18, -0.12	$0.1225\exp(-11.29\mu)+1.065\exp(-0.06412\mu)$
3	0.72, +0.08, -0.08	$0.04718\exp(-14.15\mu)+1.023\exp(-0.02347\mu)$
4	1.18, +0.09, -0.14	$0.04252\exp(-13.06\mu)+1.024\exp(-0.02386\mu)$
5	0.97, +0.03, -0.10	$0.03023\exp(-14.97\mu)+1.015\exp(-0.01515\mu)$
6	0.75, +0.19, -0.02	$0.5799\exp(-10.57\mu)+1.148\exp(-0.1408\mu)$
7	0.84, +0.07, -0.11	$0.1151\exp(-10.66\mu)+1.072\exp(-0.07029\mu)$
8	1.01, +0.03, -0.12	$1.03\exp(-12.79\mu)+1.268\exp(-0.2422\mu)$

$\mu = \frac{N_u(T)}{N_0}$, where $N_u(T)$ is the number of unfrozen droplets at temperature T, and N_0 is the total number of droplets in one freezing experiment.

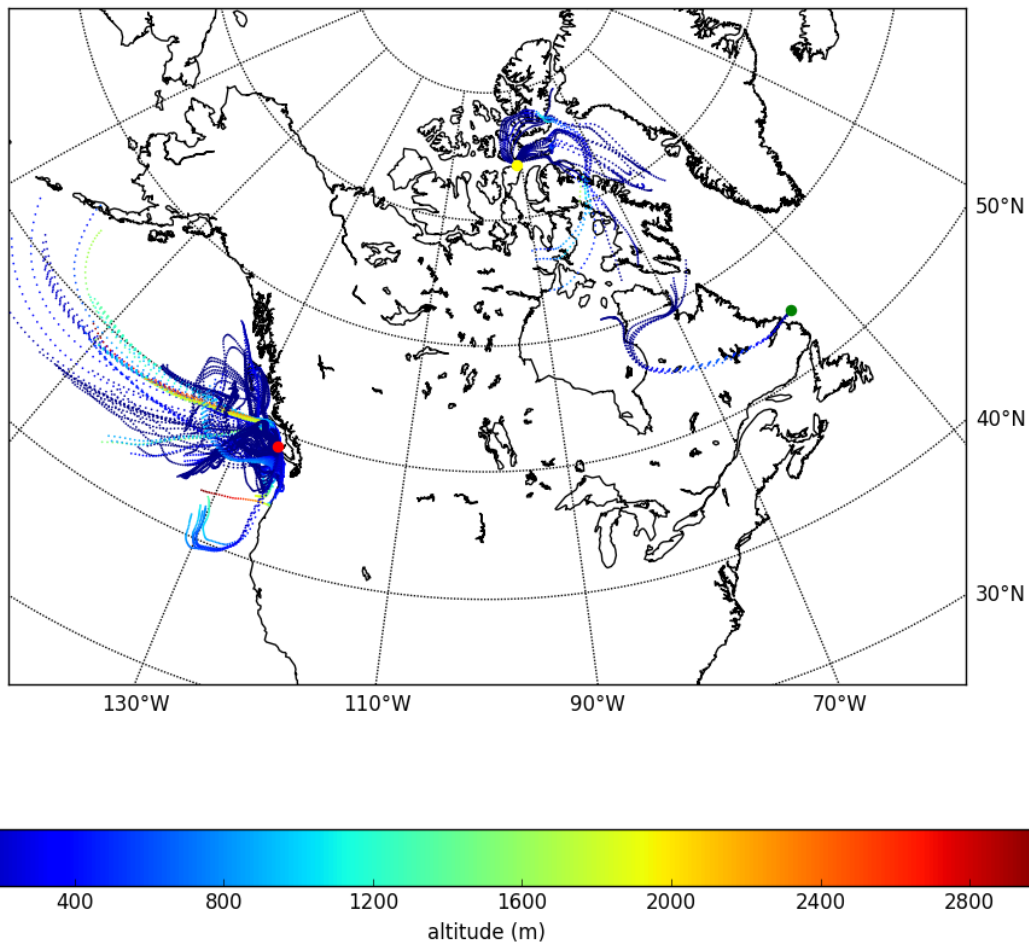


Figure S1. The 3-day HYSPLIT back trajectories initiating at 50 m above ground level for Amphitrite Point (red dot), Labrador Sea (green dot) and Lancaster Sound (yellow dot). The back trajectories were calculated for every hour during sampling period. The starting points are labeled as coloured dots, and the altitude is shown using a colour map.

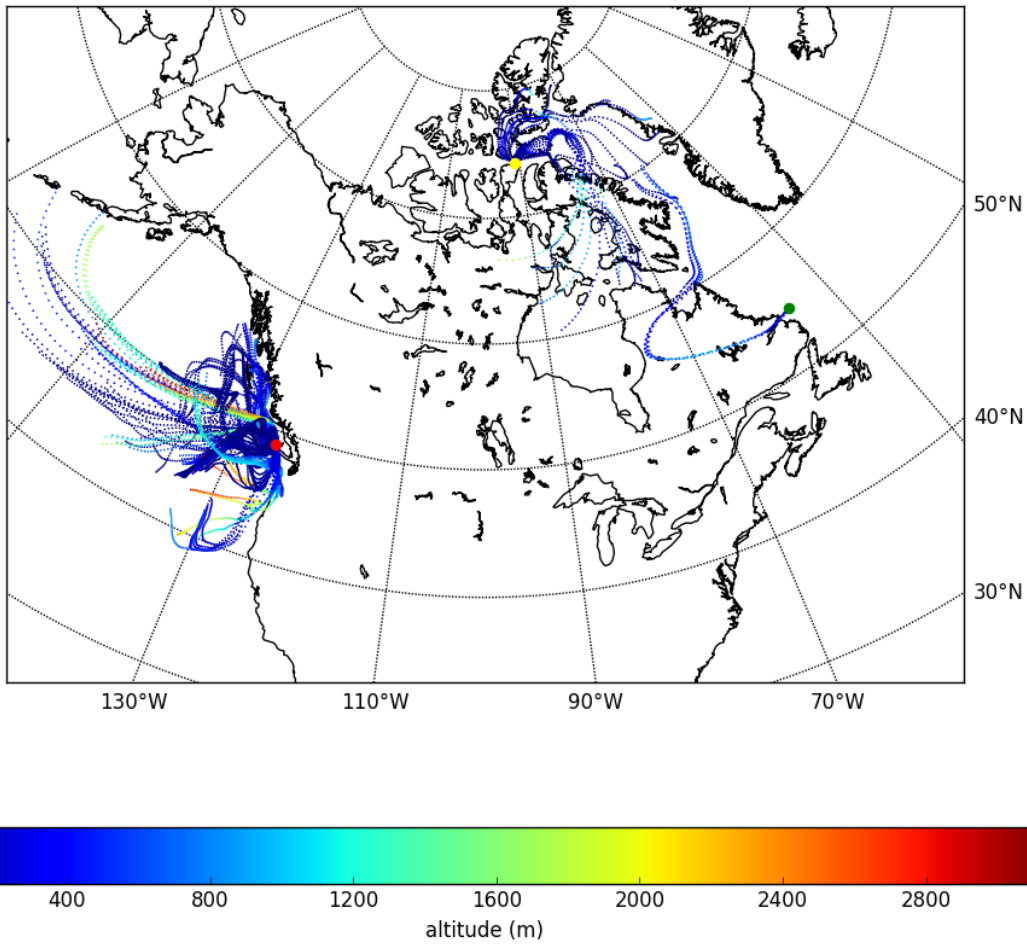


Figure S2. The 3-day HYSPLIT back trajectories initiating at 150 m above ground level for Amphitrite Point (red dot), Labrador Sea (green dot) and Lancaster Sound (yellow dot). The back trajectories were calculated for every hour during sampling period. The starting points are labeled as coloured dots, and the altitude is shown using a colour map.

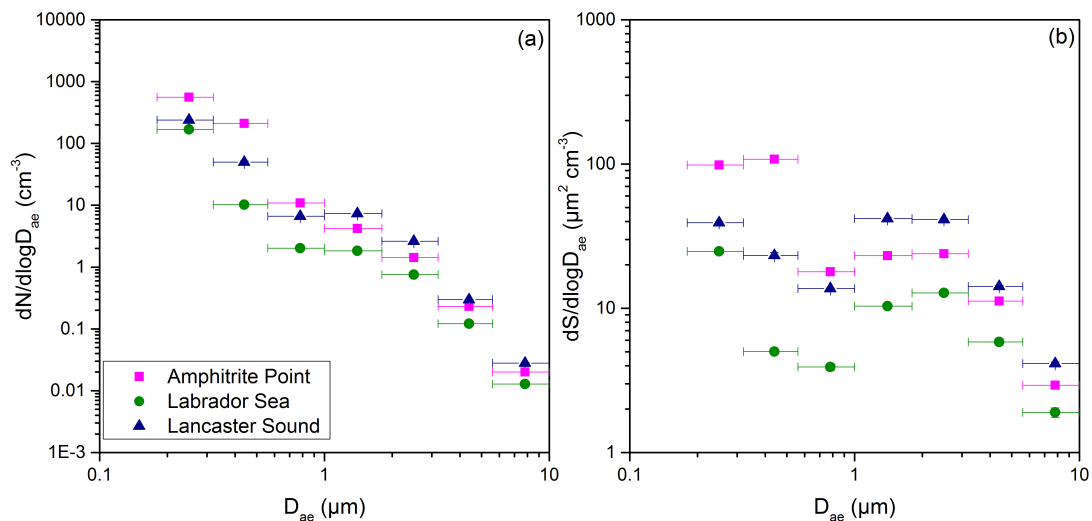


Figure S3. Concentrations of (a) aerosol number, N , and (b) surface area, S , as a function of aerodynamic diameter, D_{ae} , using the same bin widths as the MOUDI. Each data point was calculated by adding together the numbers from Fig. 4 that were within corresponding size bin. The x-error bars represent the widths of the size bins, and the y-error bars are propagated uncertainties from the error bars in Fig. 4. In most cases, the y-error bars are smaller than the size of the symbols.

5

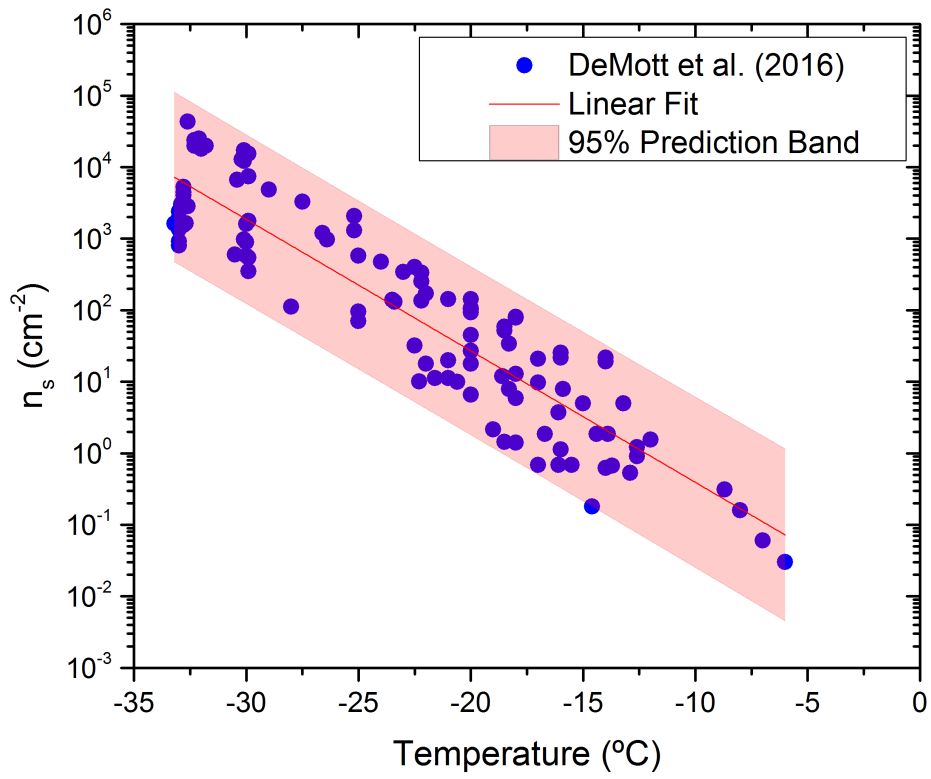


Figure S4. n_s values of sea spray aerosol as a function of temperature taken from DeMott et al. (2016). Shown is a linear fit to the data and 95% prediction bands.

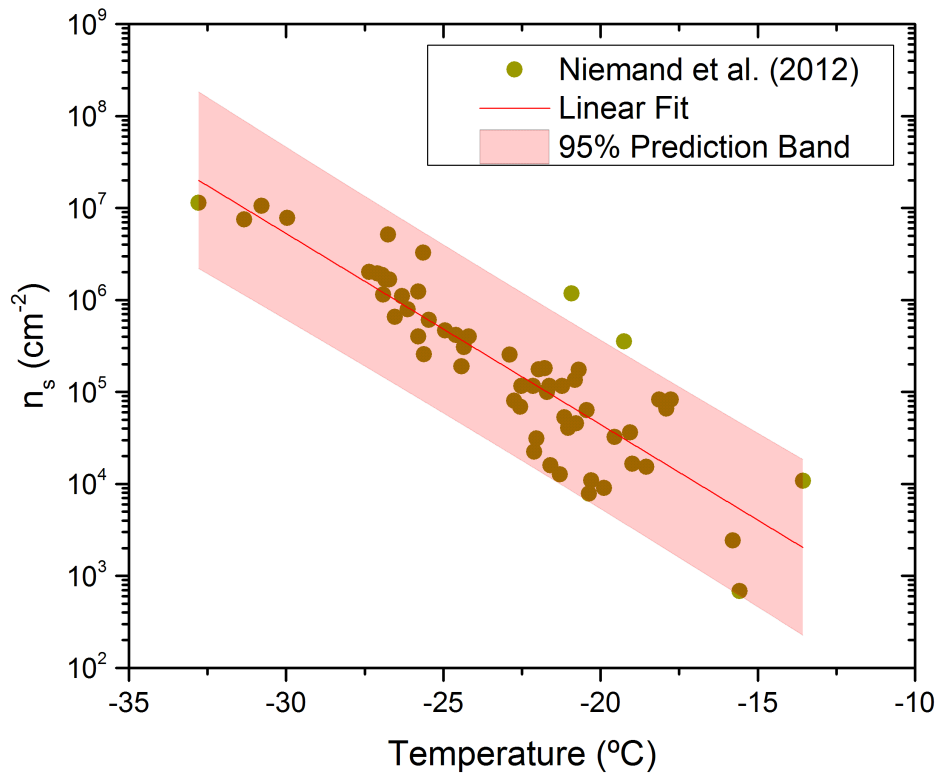


Figure S5. n_s values of mineral dust as a function of temperature taken from Niemand et al. (2012). Shown is a linear fit to the data and 95% prediction bands.